AD-A125 432 PERFORMANCE OF LASER BEAM WAVEFRONT SENSOR(U) AEROSPACE 1/1
CORP EL SEGUNDO CA AEROPHYSICS LAB C P WANG 01 FEB 83
TR-0083(3725)-1 SD-TR-83-04 F04701-82-C-0083

UNCLASSIFIED F/G 20/5 NL

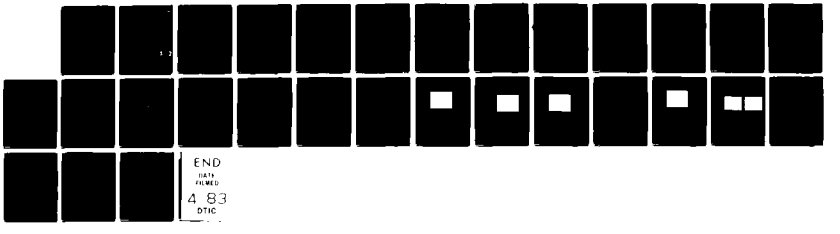

END
DATE FILMED
4 83
DTIC

M-2

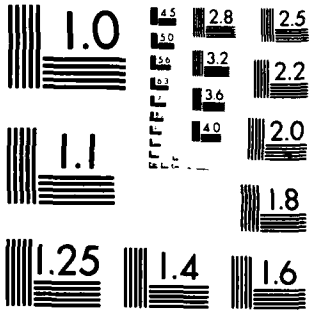

MICROCOPY RESOLUTION TEST CHART
NATIONAL BUREAU OF STANDARDS 1963 A

REPORT SD-TR-83-04

12

AD A125432

Performance of Laser Beam Wavefront Sensor

C. P. WANG
Aerophysics Laboratory
The Aerospace Corporation
El Segundo, Calif. 90245

1 February 1983

APPROVED FOR PUBLIC RELEASE;
DISTRIBUTION UNLIMITED

Prepared for

NAVAL SEA SYSTEMS COMMAND
Washington, D.C. 20362

SPACE DIVISION
AIR FORCE SYSTEMS COMMAND
Los Angeles Air Force Station
P.O. Box 92960, Worldway Postal Center
Los Angeles, Calif. 90009

DTIC
ELECTE
MAR 9 1983
S D
B

DTIC FILE COPY

83 03 09 039

This report was submitted by The Aerospace Corporation, El Segundo, CA 90245, under Contract No. F04701-82-C-0083 with the Space Division, Deputy for Technology, P.O. Box 92960, Worldway Postal Center, Los Angeles, CA 90009. It was reviewed and approved for The Aerospace Corporation by W.P. Thompson, Jr., Director, Aerophysics Laboratory. 1st Lt Steven G. Webb, Det 1, AFSTC, was the project officer for Technology.

This report has been reviewed by the Public Affairs Office (PAS) and is releasable to the National Technical Information Service (NTIS). At NTIS, it will be available to the general public, including foreign nations.

This technical report has been reviewed and is approved for publication. Publication of this report does not constitute Air Force approval of the report's findings or conclusions. It is published only for the exchange and stimulation of ideas.

Steven G. Webb, 1st Lt, USAF
Project Officer

David T. Newell, Lt Col, USAF
Actg Dir of Advanced Space Technology

FOR THE COMMANDER

Norman W. Lee, Jr., Colonel, USAF
Commander, Det 1, AFSTC

THE AEROSPACE CORPORATION

DOCUMENT CHANGE NOTICE

AD-A125 432

TO: Copyholders

DATE 3-10-83

SUBJECT: TR-0083(3725)-1
Performance of Laser Beam Wavefront Sensor
C. P. Wang

FROM J. Wittenberg
Publications

Please note that Figures 5 and 7 were transposed.

UNCLASSIFIED

SECURITY CLASSIFICATION OF THIS PAGE (When Data Entered)

REPORT DOCUMENTATION PAGE		READ INSTRUCTIONS BEFORE COMPLETING FORM
1. REPORT NUMBER SD-TR-83-04	2. GOVT ACCESSION NO. AD-A125432	3. RECIPIENT'S CATALOG NUMBER
4. TITLE (and Subtitle) PERFORMANCE OF LASER BEAM WAVEFRONT SENSOR		5. TYPE OF REPORT & PERIOD COVERED 6. PERFORMING ORG. REPORT NUMBER TR-0083(3725)-1
7. AUTHOR(s) Charles P. Wang		8. CONTRACT OR GRANT NUMBER(s) F04701-82-C-0083
9. PERFORMING ORGANIZATION NAME AND ADDRESS The Aerospace Corporation El Segundo, Calif. 90245		10. PROGRAM ELEMENT, PROJECT, TASK AREA & WORK UNIT NUMBERS
11. CONTROLLING OFFICE NAME AND ADDRESS Naval Sea Systems Command Washington, D.C. 20362		12. REPORT DATE 1 February 1983 13. NUMBER OF PAGES 27
14. MONITORING AGENCY NAME & ADDRESS(if different from Controlling Office) Space Division Air Force Systems Command Los Angeles, Calif. 90009		15. SECURITY CLASS. (of this report) Unclassified 15a. DECLASSIFICATION/DOWNGRADING SCHEDULE

16. DISTRIBUTION STATEMENT (of this Report)

Approved for public release; distribution unlimited

17. DISTRIBUTION STATEMENT (of the abstract entered in Block 20, if different from Report)

18. SUPPLEMENTARY NOTES

19. KEY WORDS (Continue on reverse side if necessary and identify by block number)

Laser Beam Quality
Wavefront Sensor
Phase Detector
Phase Profile

20. ABSTRACT (Continue on reverse side if necessary and identify by block number)

Laser beam wavefront measurement is important for laser beam quality evaluation and beam control. Reported in this paper is a laser beam wavefront sensor consisting of a phase detector and a scanner. With the use of this sensor, the wavefront phase profile across a laser beam has been obtained. The major advantages of this technique are that it is fast, sensitive, and compact. Other features are electric scanning, self-alignment, noise cancellation, and no drift. Wavefront sensor operational principles, features,

DD FORM 1473 (FACSIMILE)

UNCLASSIFIED

SECURITY CLASSIFICATION OF THIS PAGE (When Data Entered)

19. KEY WORDS (Continued)

20. ABSTRACT (Continued)

and experimental results are presented. The sensitivity of the sensor was 5 deg. This sensitivity corresponds to the change of beam quality parameter, the Strehl ratio, by 1%. Hence it is a sensitive beam quality measurement technique.

PREFACE

This work was partially supported by the Navy and by The Aerospace Corporation under its company-financed program. The author is indebted to H. Mirels for many helpful discussions, to R. L. Varwig and T. L. Felker for technical support, and to E. Turner for suggesting the parabolic mirror arrangement.

Accession For
NTIS GRA&I ☑
DTIC TAB ☐
Unannounced ☐
Justification
By
Distribution/
Availability Codes
Dist | Avail and/or Special
A

DTIC COPY INSPECTED

CONTENTS

PREFACE..... 1

I. INTRODUCTION..... 7

II. BASIC PRINCIPLES..... 9

III. MECHANICAL SCANNING WITH A PARABOLIC MIRROR..... 13

IV. EXPERIMENTAL RESULTS..... 17

V. CONCLUSION..... 27

REFERENCES..... 29

PRECEDING PAGE BLANK-NOT FILMED

FIGURES

1. Schematic of the Phase Detector..... 10

2. Schematic of the Parallel Scanner..... 14

3. Experimental Setup..... 18

4. Calibration of Phase Detector..... 20

5. Intensity and Phase Profile Across the Laser Beam..... 21

6. Laser Beam Intensity Profile After Spatial Filter..... 22

7. Intensity and Phase Profile with a 1-mm-diameter Wire in the Middle of the Beam..... 24

8. Intensity and Phase Profiles Without Spatial Filter and with Spatial Filter..... 25

PRECEDING PAGE BLANK-NOT FILMED

I. INTRODUCTION

Conventional wavefront measuring devices such as the shearing interferometer[1,2] are difficult to use and have low frequency response. In these instruments, a laser beam is split into two separate beams, which are then recombined by means of beam splitters and mirrors. Upon recombination, fringes are formed that mark the phase difference introduced as a result of each beam traveling a different path. Fringe distortion is a measure of wavefront distortion. Such techniques have been used for wavefront measurement for testing optical surfaces and lenses.[2] In addition, the shearing interferometer has been used to observe laser beam quality and to measure wavefront deformation and phase fluctuation in a laser beam that propagates through a turbulent medium.[3,4] However, because many beam splitters and mirrors are used, the shearing interferometer is very difficult to align; the measurement is made over a relatively long time period and is susceptible to environmental noise and vibration.[5]

Reported in this paper is a wavefront sensor using acousto-optic modulator and heterodyne techniques[6] and parallel scanning using a parabolic mirror. The major advantages of this wavefront sensor are that it is fast, sensitive, and compact. Other features are self-alignment, noise cancellation, lack of drift, and a possibility of electronic scanning. This technique has been successfully applied for the measurement of phase fluctuation,[6] fine steering angle,[7] small displacement,[8,9] and laser beam wavefront perturbations.*

*C. P. Wang, "Laser Beam Wavefront Sensor Using AO Modulator and Heterodyne Technique," to be presented in Laser '82 Conference, New Orleans, December 13-17, 1982.

Other possible applications are to improve boresight accuracy,* pointing and tracking stability, and laser alignment. This technique can also be used as a discriminator for adaptive optics[10] or an active resonator.

*C. P. Wang and J. M. Bernard, "Application of Wavefront Sensors to Improve the Talon Gold Pointing Telescope Boresight Accuracy," Aerospace ATM-80(6755)-2, October 23, 1980.

II. BASIC PRINCIPLES

A detailed description of the operational principles of the wavefront sensor is given in Ref. 6. Briefly, the sensor consists only of an acousto-optic modulator and a small area detector, as shown in Fig. 1. The acousto-optic modulator acts as a moving phase grating. A diffraction pattern is obtained by the propagation of a plane parallel, monochromatic light beam of wavelength λ through the acoustic field whose wavelength is Λ.

Light in the higher diffraction orders has vector components along the axis of sound propagation and therefore experiences a frequency shift as a result of the Doppler effect. For traveling acoustic waves, the shifted frequencies ω_N are

$$\omega_N = \omega \pm N\Omega \tag{1}$$

where ω and Ω are the light frequency and acoustic frequency, respectively, and $N = 0, 1, 2 \ldots$ is the order of the diffraction. The diffraction angles θ_N are

$$\text{Sin } \theta_N = N \frac{\lambda}{\Lambda} \tag{2}$$

The signal resulting from moving fringes (i.e., beat signal) at the photodetector is then

$$I_p(t) = A \cos \left[\Omega t - \Delta\phi(t) + B\right] \tag{3}$$

where A is the amplitude of the beat signal, B is a constant phase, and $\Delta\phi$ is the phase difference between points X_o and X_1.

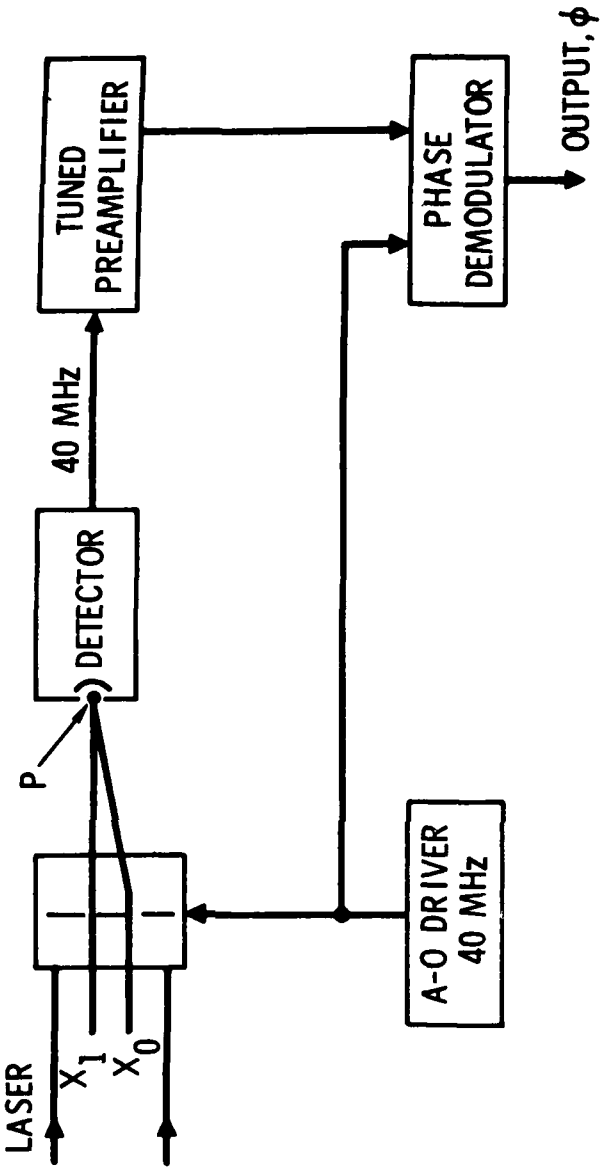

Fig. 1. Schematic of the Phase Detector.

It is clear from Eq. (3) that the beat signal is equivalent to a phase-modulated signal whose carrier frequency equals the frequency of the acoustic waves. When this beat signal is fed into a phase demodulator, we can immediately receive its phase difference $\Delta\phi(t)$.

A schematic block diagram of the laser beam phase detector is shown in Fig. 1. Here the acousto-optic modulator driver signal is used as a reference for the phase demodulator. Therefore, any drift in frequency is canceled, and accurate, relative phase measurements are achieved.

III. MECHANICAL SCANNING WITH A PARABOLIC MIRROR

As shown in Eq. (3), the phase detector measures the relative phase at two fixed points. To obtain the phase distribution across a laser beam, a scanning mirror could be used to move the laser beam across the phase detector. The measured relative phase is very sensitive to the laser beam incident angle. To minimize the variation of this incident angle, a parabolic mirror with a scanning (rotating) mirror at the focus was employed. As shown in Fig. 2, a scanning mirror at the focus scans the collimated beam in a parallel manner across the phase detector. Furthermore, because of disturbances, near-field intensity and phase profiles could be obtained by generating the disturbances at the conjugate plane of the phase detector.

A first order estimate of the required alignment accuracy was made. The results indicate that the phase variation $\Delta\alpha$, because of a small error in locating the scanning mirror at the focal point, is very large, i.e.,

$$\Delta\alpha \sim \frac{\Delta X}{F} \cdot \frac{d}{\lambda} \cdot \frac{D}{2F} \sim \frac{\Delta y}{F} \frac{d}{\lambda} \tag{4}$$

where ΔX and Δy are deviations (from the focal point) along the optical axis and perpendicular to the optical axis of the parabolic mirror, respectively, D and F are the diameter and focal length of the parabolic mirror, respectively, and d is the beam diameter. For a flat mirror,

$$\Delta\alpha \sim \frac{S}{F} \frac{d}{\lambda} \tag{5}$$

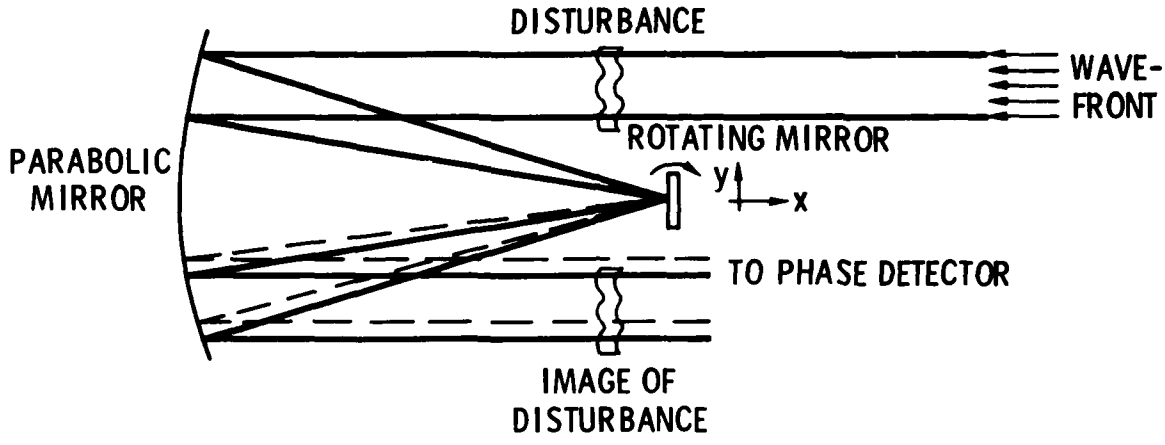

Fig. 2. Schematic of the Parallel Scanner.

where S is the separation between the two points where relative phase difference was measured. If we require the parabolic mirror to perform much better than a flat mirror, then we require

$$\Delta y \ll S, \ \Delta X \ll \frac{2F}{D} S \tag{6}$$

Usually, $F/D > 1$, hence the alignment in the direction perpendicular to the optical axis is more critical. For the experiment reported here, $F = 1.5$ m, $D = 25$ cm, and $S = 2.5$ mm. So, Δy should be less than a fraction of 1 mm.

Because the HF laser is invisible, it is rather difficult to align. Hence a HeNe laser was used to align the optics. The alignment laser beam was first focused by a 25× objective lens and then passed through a 25-μm pinhole located at the focus of the parabolic mirror. The beam reflected from the parabolic mirror became parallel. The HF laser beam is then aligned to be coincident with the HeNe laser beam. The alignment was completed, and the pinhole was replaced by the scanning mirror. Final alignment was achieved by minimizing the measured $\Delta\alpha$ by adjusting the position of the scanning mirror and the direction of the incoming HF laser beam. As shown in the next section, $\Delta\alpha < 5$ deg has been achieved.

IV. EXPERIMENTAL RESULTS

The experimental setup consists of a continuous-wave (cw) HF chemical laser, a spatial filter and beam expander, a parabolic mirror, a scanning mirror, an acousto-optic modulator, and a photodetector, as shown in Fig. 3. The cw HF chemical laser was described in Ref. 11. Briefly, the gain medium was 30 cm long with single-line output $P_2(7)$ (at 2.8705 μm) of 8 W. A stable resonator was used, consisting of a 3-m radius-of-curvature total reflection and a flat grating as the output coupling. The resonator mirrors were separated by a distance L of 60 cm.

A TEMoo-mode output beam was obtained with a beam diameter of 2.2 mm and a far-field divergence angle of 1.75 mrad. The output beam was fed to a 10× beam expander; the final beam diameter at the collimating mirror was about 30 mm. The spatial filter consisted of a 5-cm focal length ZnSe lens and a 0.1 mm pinhole. A 1-m radius of curvature and 2.5-cm-diameter concave mirror was used to collimate the beam. The parabolic mirror used had a 25-cm diameter and 1.5-m focal length. The scanning mirror was a small mirror mounted on an electro-mechanical scanner.

The laser beam then impinged on an acousto-optic modulator. The clear aperture of the acousto-optic modulator was 5 × 25 mm, with the traveling acoustic waves propagating along the 25-mm aperture direction. The acousto-optic interaction length was 24 mm. An 8-W radio frequency (RF) power amplifier with center frequency at 40 MHz drives the acousto-optic modulator. The intensity ratio of first order to zero order was about 0.3. The diffraction angle θ was 1.2 deg at Ω = 40 MHz.

16 atoms

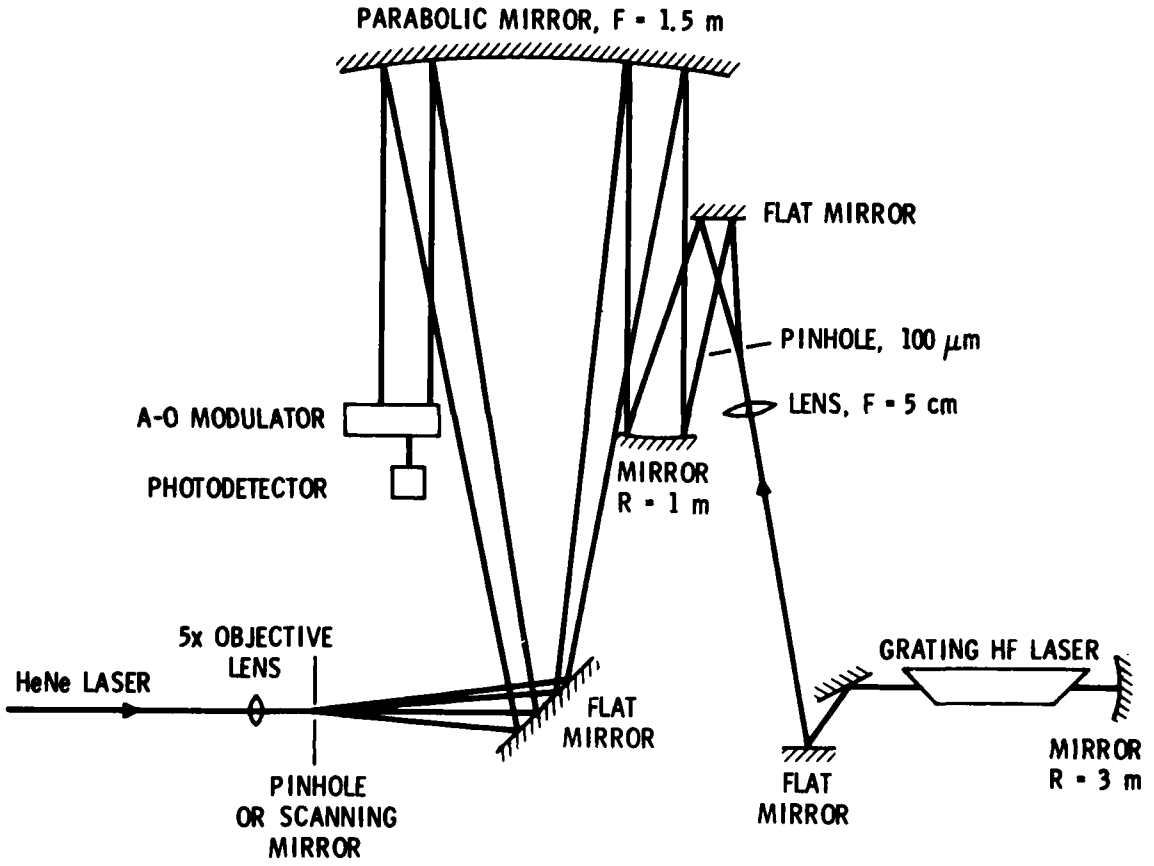

Fig. 3. Experimental Setup.

A fast, room-temperature InAs detector was placed 10 cm behind the acousto-optic modulator. The detector area was 0.14×0.14 mm^2, and the detectability D* was about 10^8 cm Hz$^{1/2}$/W at room temperature. The detector output was fed to a tuned amplifier and then to the phase demodulator. The sensitivity of the phase demodulator was set at 22.5 deg/V, and the dynamic range at 180 deg.

To calibrate the phase detector, the parabolic mirror was replaced by a flat total reflector. Then the beam steering angle could be obtained by measuring the scanning mirror driver voltage, as shown in Fig. 4. In this figure, the top trace is the center portion of the laser beam profile, the middle trace is the corresponding phase detector output, and the bottom trace is the scanning mirror driver voltage. The shape of both the mirror driver voltage and the phase detector output was very similar. This assured the linear relationship as expected. The measured calibration constant agreed with the theoretical calculation very well.

For parallel scanning, the flat mirror was then replaced by the parabolic mirror. The intensity and phase profile across the laser beam is shown in Fig. 5. The intensity was a truncated Gaussian profile. Although the beam profile was nearly Gaussian (see Fig. 6) after the spatial filter, the collimating mirror was only 25 mm in diameter whereas the laser beam diameter was nearly 30 mm at the collimating mirror. Hence only the center portion of the beam was reflected by the collimating mirror. The ripple on the intensity profile is the result of mirror edge diffraction effects. The phase demodulator will not track when the signal is below a certain level. Hence only the center portion of the lower trace in Fig. 5 is meaningful. The signal outside

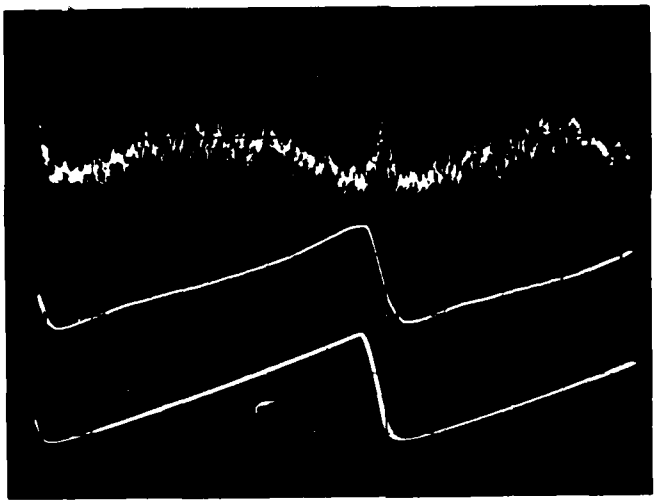

Fig. 4. Calibration of Phase Detector. Upper trace: intensity profile, 2 V/div; middle trace: relative phase, 112.5 deg/div; lower trace: driver voltage, 120 deg/div; sweep speed, 20 msec/div.

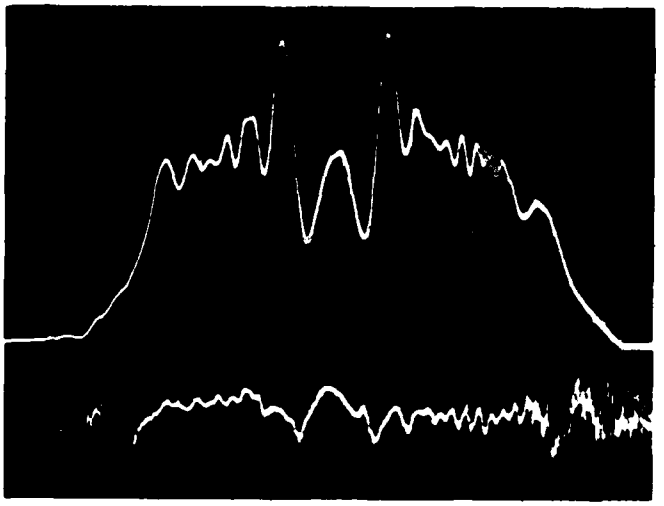

Fig. 5. Intensity and Phase Profile Across the Laser Beam. Upper trace: intensity profile, 2 V/div; lower trace: phase profile, 112.5 deg/div; sweep speed, 2 msec/div.

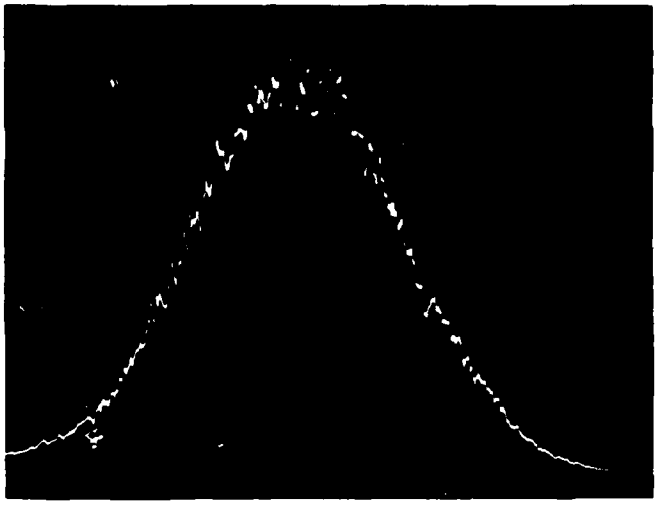

Fig. 6. **Laser Beam Intensity Profile After Spatial Filter.** Intensity profile, 0.3 V/div; sweep speed, 0.5 msec/div.

of the beam profile consists of RF noise. The noise level inside of the beam profile was about 5 deg because of the detector noise and RF pickup. Further improvement on those noises could be achieved by properly grounding and shielding. Also, narrowband filter could be used to reduce the noise. However, this would also reduce the frequency response of the sensor.

The constant phase signal in the center of Fig. 5 indicates that the beam has been scanned in a parallel manner, i.e., the steering angle was almost zero. However, there are small phase fluctuations resulting from mirror edge diffraction effect. This demonstrated that a sensitive, measurable phase variation of 5 deg wavefront measurement has been achieved.

To further examine the effect of diffraction, a 1-mm-diameter metal wire was placed in the middle of the beam at a position between the collimating mirror and the parabolic mirror, i.e., at the conjugate plane of the phase detector. The measured intensity and phase profile are shown in Fig. 7. Large intensity and phase changes have been observed. This qualitatively agrees with the Fresnel diffraction theory.[12]

To examine the effect of a spatial filter, a 5× beam expander with and without a pinhole was used. The intensity and phase profiles without and with spatial filter are shown in Fig. 8a and 8b, respectively. The spatial filter clearly removed the ripples on both intensity and phase profiles.

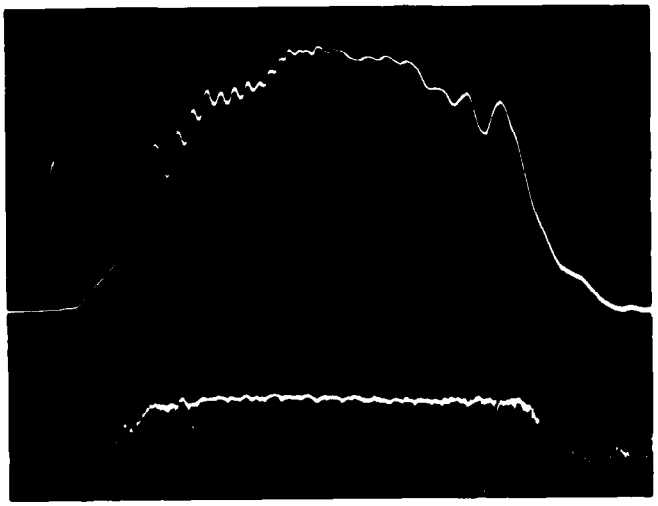

Fig. 7. Intensity and Phase Profile with a 1-mm-Diameter Wire in the Middle of the Beam. Upper trace: intensity profile, 2 V/div; lower trace: phase profile, 45 deg/div; sweep speed, 2 msec/div.

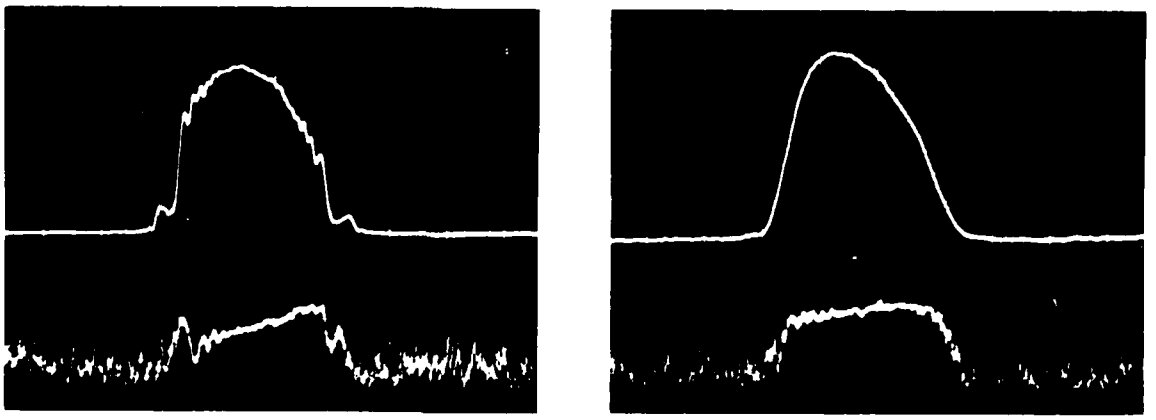

Fig. 8. Intensity and Phase Profiles (a) Without Spatial Filter and (b) with Spatial Filter. Upper trace: intensity profile, 2 V/div (a), 1.5 V/div (b); lower trace: phase profile, 45 deg/div; sweep speed, 1 msec/div.

V. CONCLUSION

In conclusion, we have demonstrated that sensitive wavefront measurement could be achieved by the acousto-optic modulator and heterodyne technique. The phase profile of a wavefront across the laser beam could also be obtained by using this technique, together with a mechanical scanner and a parabolic mirror. All these techniques are important for laser beam control and beam quality study.

Finally, for laser beam quality measurement, the Strehl ratio or Strehl intensity has often been used, which is the ratio of intensities with and without aberrations.[12] Based on the calculation in Ref. 12, there is a 1% decrease in Strehl ratio for a root-mean-square (rms) phase aberration of 5 deg. This indicated that the wavefront sensor is a sensitive beam quality measurement technique.

REFERENCES

1. O. Bryngdahl, "Applications of Shearing Interferometer," Prog. in Opt. 6, 37-83 (1965).

2. J. H. Bruning, D. R. Herriott, J. E. Gallagher, D. P. Rosenfield, A. D. White, and D. J. Brangaccio, "Digital Wavefront Measuring Interferometer for Testing Optical Surfaces and Lasers," Appl. Opt. 13, 2693-2703 (1974).

3. D. Kelsall, "Optical Seeing Through the Atmosphere by an Interferometer Technique," J. Opt. Soc. Am. 63, 1472-1484 (1973).

4. M. V. R. K. Murty, "A Compact Lateral Shearing Interferometer Based on the Michelson Interferometer," Appl. Opt. 9, 1146-1148 (1970).

5. J. Van Workmen, Z. A. Plascyk, and M. L. Skolnick, "Laser Wavefront Analyzer for Diagnosing High-Energy Lasers," Opt. Engineering 18, 187-193 (1979).

6. C. P. Wang and R. L. Varwig, "Measurement of Phase Fluctuations in a HF Chemical Laser Beam," J. Appl. Phys. 50, 7917-7920 (1979).

7. C. P. Wang and R. L. Varwig, "Direct Measurement of Anomalous Dispersion by Beam Steering and a Wavefront Sensor," Appl. Phys. Lett. 39, 374-376 (1981).

8. R. L. Varwig, R. L. Sandstrom, and C. P. Wang, "Calibration of Piezoelectric-Driven Mirrors for Laser Resonators," Rev. Sci. Instr. 52, 200-203 (1981).

9. C. P. Wang, R. L. Varwig, and P. J. Ackman, "Measurement and Control of Subangstrom Mirror Displacement by Acousto-optical Technique," Rev. Sci. Instr. 53, 963-966 (1982).

28 Blank

10. J. G. R. Hansen, R. M. Richard, and R. R. Shannon, "Deformable Primary Mirror for a Space Telescope," Appl. Opt. 21, 2620-2630 (1982)

11. C. P. Wang, "Frequency Stability of a cw HF Chemical Laser," J. Appl. Phys. 47, 221-223 (1976).

12. Born and Wolf, "Principles of Optics," Chapts. VIII and XI, Pergamon, N.Y. (1970).

☆ U.S. Government Printing Office 1983 683-004/2124

LABORATORY OPERATIONS

The Laboratory Operations of The Aerospace Corporation is conducting experimental and theoretical investigations necessary for the evaluation and application of scientific advances to new military space systems. Versatility and flexibility have been developed to a high degree by the laboratory personnel in dealing with the many problems encountered in the nation's rapidly developing space systems. Expertise in the latest scientific developments is vital to the accomplishment of tasks related to these problems. The laboratories that contribute to this research are:

Aerophysics Laboratory: Launch vehicle and reentry aerodynamics and heat transfer, propulsion chemistry and fluid mechanics, structural mechanics, flight dynamics; high-temperature thermomechanics, gas kinetics and radiation; research in environmental chemistry and contamination; cw and pulsed chemical laser development including chemical kinetics, spectroscopy, optical resonators and beam pointing, atmospheric propagation, laser effects and countermeasures.

Chemistry and Physics Laboratory: Atmospheric chemical reactions, atmospheric optics, light scattering, state-specific chemical reactions and radiation transport in rocket plumes, applied laser spectroscopy, laser chemistry, battery electrochemistry, space vacuum and radiation effects on materials, lubrication and surface phenomena, thermionic emission, photosensitive materials and detectors, atomic frequency standards, and bioenvironmental research and monitoring.

Electronics Research Laboratory: Microelectronics, GaAs low-noise and power devices, semiconductor lasers, electromagnetic and optical propagation phenomena, quantum electronics, laser communications, lidar, and electro-optics; communication sciences, applied electronics, semiconductor crystal and device physics, radiometric imaging; millimeter-wave and microwave technology.

Information Sciences Research Office: Program verification, program translation, performance-sensitive system design, distributed architectures for spaceborne computers, fault-tolerant computer systems, artificial intelligence, and microelectronics applications.

Materials Sciences Laboratory: Development of new materials: metal matrix composites, polymers, and new forms of carbon; component failure analysis and reliability; fracture mechanics and stress corrosion; evaluation of materials in space environment; materials performance in space transportation systems; analysis of systems vulnerability and survivability in enemy-induced environments.

Space Sciences Laboratory: Atmospheric and ionospheric physics, radiation from the atmosphere, density and composition of the upper atmosphere, aurorae and airglow; magnetospheric physics, cosmic rays, generation and propagation of plasma waves in the magnetosphere; solar physics, infrared astronomy; the effects of nuclear explosions, magnetic storms, and solar activity on the earth's atmosphere, ionosphere, and magnetosphere; the effects of optical, electromagnetic, and particulate radiations in space on space systems.